Havu, Paula; Blum, Volker; Havu, Ville; Rinke, Patrick; Scheffler, Matthias

Large-scale surface reconstruction energetics of Pt(100) and Au(100) by all-electron density functional theory

Published in:
Physical Review B

DOI:
10.1103/PhysRevB.82.161418

Published: 01/01/2010

Document Version
Publisher's PDF, also known as Version of record

PHYSICAL REVIEW B **82**, 161418(R) (2010)

Large-scale surface reconstruction energetics of Pt(100) and Au(100) by all-electron density functional theory

Paula Havu,[1,*] Volker Blum,[1] Ville Havu,[1,2] Patrick Rinke,[1] and Matthias Scheffler[1]
[1]*Fritz-Haber-Institut, Berlin, Germany*
[2]*Department of Applied Physics, Aalto University, Helsinki, Finland*
(Received 25 September 2010; published 25 October 2010)

The low-index surfaces of Au and Pt all tend to reconstruct, a fact that is of key importance in many nanostructure, catalytic, and electrochemical applications. Remarkably, some significant questions regarding their structural energies remain even today, specifically for the large-scale quasihexagonally reconstructed (100) surfaces: rather dissimilar reconstruction energies for Au and Pt in available experiments and experiment and theory do not match for Pt. We here show by all-electron density functional theory that only large enough "$(5\times N)$" approximant supercells capture the qualitative reconstruction energy trend between Au(100) and Pt(100), in contrast to what is often done in the theoretical literature. Their magnitudes are then in fact similar and closer to the measured value for Pt(100); our calculations achieve excellent agreement with known geometric characteristics and provide direct evidence for the electronic reconstruction driving force.

DOI: 10.1103/PhysRevB.82.161418 PACS number(s): 68.35.B−, 68.35.Md, 71.15.Mb, 73.20.At

The late 5*d* transition metals Pt and Au and their surfaces are of central importance for a wide variety of applications, including catalysis, electrochemistry, substrates for nanostructure creation and characterization, etc. (some recent examples are discussed as Refs. 1–21, below). Their low-index surfaces (100), (110), and (111) are paradigm systems to understand catalytic and electrochemical processes at the atomic scale, to the point that only textbooks and handbooks (e.g., Refs. 1 and 2) attempt somewhat comprehensive overviews. Au(111), (100), and Pt(100) are ubiquitous as substrates for nanostructure creation and manipulation both due to their relative inertness and due to the fact that they tend to form well-defined, large-scale *quasihexagonal* ("hex") surface reconstructions[22–27]—not just *in vacuo* but also in solutions under electrochemical adsorption[3] and epitaxial growth conditions.[4,5] The reconstructions imply a significant rearrangement of surface atoms and a creation of qualitatively distinct surface areas[28,29] [fcc/hcp stacking for (111), steeper vs flatter ridges for (100)]. These local structure variations in Au and Pt (100) and (111) surfaces are the key ingredient for subsequent nanostructure growth and processes on top, e.g., by way of a preferential nucleation of deposits (Refs. 6–10 and references therein). To give some recent examples where this atomic structure is important: the formation of magnetic structures,[7,11] self-assembled nanostructured arrays of (bio)molecules,[12] magnetic dots[8] or supramolecules,[13,14] the structural and electronic underpinnings of catalytic reactivity,[3,6,15] on-surface synthesis of well-separated molecular wires[16] for transport studies,[16,17] well-defined patterns of molecular switches,[18,19] or atomic-scale visualization of kinetics and dynamics of surface processes.[4,5,20,21] The balance of reconstruction/deconstruction can be essential for chemical processes (Refs. 3 and 15 and references therein); for instance, the peak of catalytic activity of Pd/Au(100) occurs at a coverage of 0.07 ML,[30] precisely in the range where one would expect reconstruction/deconstruction to occur.[10,31]

In order to obtain a truly predictive theoretical understanding of these phenomena, one would ideally like to use current first-principles theory for "realistic enough" unit-cell sizes. However, this endeavor faces a significant obstacle: the sheer surface reconstruction size necessitates that even very recent studies employ instead much smaller model supercells.[12,13] This obstacle is most pronounced for the (100) surfaces, whose quasihexagonal superstructures are almost uniformly contracted compared to bulk (111) planes [25% more atoms per area in the hex layer than in a bulklike (100) plane] and are, strictly, incommensurate with the underlying square substrate.[28,29,32–36] *In vacuo*, they are additionally slightly rotated $(0.5°-1°)$ against the nominal (100) surface rows[32,35–38] but the exact hex layer geometry and surface conditions are interrelated: on stepped surfaces, periodicities change,[39] and at high temperature[35,36,38] or under catalytic conditions,[3] unrotated hex planes are observed. Again, this would not be a grave obstacle for either current experiments or theory if suitably accurate, small periodic approximants for the full surface structure could be found. However, it turns out that the smallest approximants which cover all key features (two-dimensional lateral contraction, rotation, and differently buckled qualitative surface areas) are already significant in size: roughly speaking, "$(5\times N)$,"[23,37,38,40] where $N\approx 20-30$, i.e., ≥ 100 atoms to be considered in each layer.

The primary point of the present Rapid Communication is to demonstrate, from first principles, that indeed large-scale $(5\times N)$, and not smaller approximants to the Au(100) and Pt(100) quasihexagonal reconstructions are essential to obtain the qualitatively correct surface structural energetics from first principles. Our results are based on a numerically converged all-electron description, using density functional theory (DFT) in the local-density approximation (LDA) and PBE (Ref. 41) generalized-gradient approximation. While computationally challenging, such a description is now feasible. In addition, it provides a key benchmark for any computationally cheaper, more approximate methods to be used.

Concerning the reconstruction energy and driving force, some significant *qualitative* lessons can already be learned from simple (1×1) surface models. Using DFT-LDA, Takeuchi, Chan, and Ho (TCH) (Ref. 42) demonstrated that

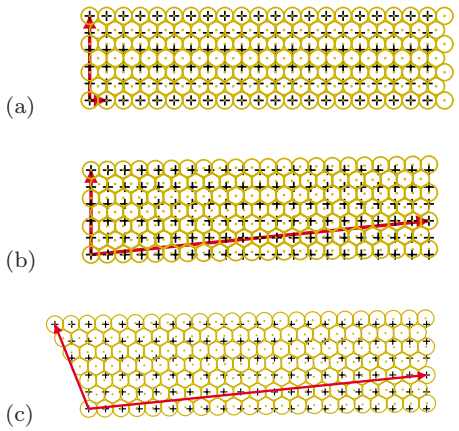

FIG. 1. (Color online) Structure and distortion of the quasihexagonal layer. Circles: topmost (hex) layer, crosses: second (square) layer. Unit vectors of the coincidence lattice of both planes are shown by arrows. (a) (5×1) and (b) (5×20) superstructure. The hex layer is compressed by 4% with respect to bulk (111) in both dimensions and rotated by 1° in one dimension. (c) (5×20)-type superstructure, rotated in both dimensions.

free-standing Au(111) planes achieve a large energy lowering when uniformly contracted to the interatomic spacing of the Au(100) hex reconstruction. Using a Frenkel-Kontorova model, TCH found a net surface energy gain through reconstruction, albeit very small: $\Delta E_{\text{hex}}<0.01$ eV per unit area of the (100) surface [eV/1×1]. This is not far from an experimental, electrochemical estimate [0.02 eV/1×1 (Ref. 43)], but, puzzlingly, smaller by a factor ≈6 than a careful assessment of the reconstruction energy of Pt(100) *in vacuo*, 0.12 eV/1×1 (Ref. 44) [an earlier analysis placed Pt(100) even higher, at 0.21 eV/1×1].[45,46] Adding to the confusion is the fact that theoretical estimates for Pt(100) based on small (5×1) approximant cells *in vacuo* yield only half the experimental value (0.05–0.07 eV/1×1).[47–49] For Au(100), (5×1)-based theoretical estimates[50–52] are approximately in line with the electrochemical experiments. Since Au(100) and Pt(100) do behave similarly also regarding thermal stability,[35,36] one might consider the experimental reconstruction energy estimate for Pt(100) an outlier—if it were not for the fact that it is this experiment which pertains to the full reconstruction in the vacuum environment, and not to an electrochemical environment, or to a restricted unit cell. Remarkably, our calculations of the full $(5\times N)$ reconstruction energy resolve this puzzle in favor of the Pt(100) experiment[44] and show that both the experimental and earlier theoretical values for Au(100) (Refs. 50–52) underestimate the reconstruction energy *in vacuo*.

In retrospect, it might seem unsurprising that a full supercell treatment should resolve such differences but it is important to note that this result was not predictable. In light of the noticeable differences of the first experimental data shown in Refs. 45 and 46, and later data shown in Ref. 44, it was not at all clear whether further experimental modifications or better theory were needed. We now resolve this question unambiguously.

Figure 1 shows the unit cells of the specific approximants that are important for this work. In each case, the hexagonal top layer (circles) is slightly distorted to form a commensurate coincidence lattice (arrows) with the underlying square substrate (crosses). Figure 1(a) shows the popular (5×1) approximant. Compared to an ideal hexagonal layer, the top layer is compressed by 4% in one dimension but not in the other. To account for the reconstruction in both dimensions, larger $(5\times N)$-type approximants ($N\approx20-30$) are needed. In Fig. 1(b), the hexagonal plane is thus compressed in *both* dimensions and somewhat distorted so that its close-packed rows are additionally rotated by ≈1° against the substrate. Finally, Fig. 1(c) shows a closely related $(5\times N)$-type approximant with a rotation of ≈1° in both dimensions. We model the hex layers as part of five-layer slabs (two layers relaxed, three kept fixed in bulk positions) that are separated by more than 25 Å of vacuum. The largest slabs ($N=40$) thus comprise 1046 atoms, 446 of which are fully relaxed. We emphasize that this number refers to heavy elements, no pseudoization is employed, metallic systems are not amenable to current $O(N)$ methods, and that especially transition-metal slabs can be subject to serious self-consistency instabilities (charge sloshing).[53] On the methodological side, our work therefore reflects significant efforts toward scalability and efficiency (including a real-space version of Kerker preconditioning[54]) in our accurate "DFT and beyond" code FHI-aims,[54,55] which was used throughout this work on massively parallel hardware (IBM's BlueGene/P) and on a recent, Infiniband-connected Sun Microsystems Linux cluster.

Compared to a (1×1) layer, a $(5\times N)$ plane ($N>1$) contains $(N+5+1)$ additional atoms in the unit cell. In terms of total energies for individual surface slabs, E^{slab}, and the total energy per atom in the bulk, $E^{\text{atom,bulk}}$, the reconstruction energy $\Delta E_{5\times N}$ (here defined to be positive if a reconstruction is favored) is

$$-\Delta E_{5\times N}=E^{\text{slab}}_{5\times N}-5NE^{\text{slab}}_{1\times1}-(N+6)E^{\text{atom,bulk}}. \quad (1)$$

For all energies in this work, we chose accurate computational settings to guarantee a cumulative error of $\Delta E_{5\times N}$ below 0.02 eV/(1×1) at most. Technical choices and convergence tests are summarized in Ref. 56, which is the supporting material submitted with this work.

Figure 2 summarizes our results regarding $\Delta E_{5\times N}$ for Pt(100) and Au(100), using the approximant cells Figs. 1(a) and 1(b). Since the density of $(5\times N)$ planes increases as N decreases, we plot $\Delta E_{5\times N}$ as a function of the *lateral atomic packing density* relative to the underlying (100) lattice: $\theta=n_{\text{hex}}/n_{100}$. Experimentally, surface X-ray diffraction (SXRD) yields $\theta\approx1.242-1.250$ for Pt(100) (Refs. 35 and 36) and 1.259 for Au(100).[33,35] We find that the *two-dimensional* $(5\times N)$ compression is indeed energetically favored over (5×1) both in LDA and PBE. In essence, the energy surface shows shallow minima that are precisely in line with the experimental analysis. The experimental trend of a denser hex layer for Au than for Pt is clearly confirmed. For Pt, the energy gain of $(5\times N)$ over (5×1) is small (~0.01 eV/1×1) but Au roughly *doubles* its reconstruction energy. This change brings the reconstruction energies of both surfaces close to one another and also to the experimental reconstruction energy estimate for Pt(100). In numbers, we find $\Delta E_{5\times N}=0.07$ eV/1×1 (Au) vs 0.10 eV/1×1 (Pt)

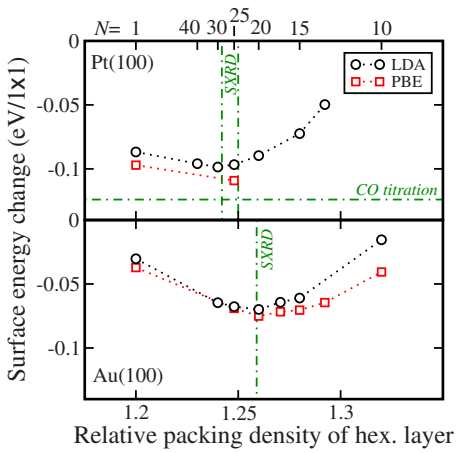

FIG. 2. (Color online) Change in surface energy with reconstruction, compared to (1×1) [negative of $\Delta E_{5\times N}$, Eq. (1)], for Pt(100) (upper panel) and Au(100) (lower panel) using DFT-LDA/PBE, as a function of the lateral atomic packing density θ. Dashed-dotted lines: experimental estimates for the packing density from SXRD, (Refs. 35 and 36) and for the Pt(100) reconstruction energy from the reanalysis (Ref. 44) of CO titration calorimetry data (Refs. 45 and 46).

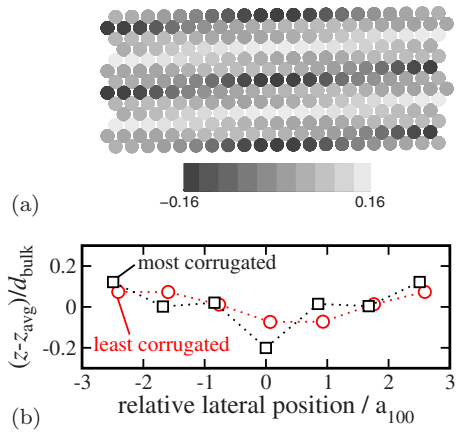

FIG. 3. (Color online) (a) Top view of the hex layer on an Au(100)-(5×20) reconstruction model (LDA). z coordinates of all atoms are in different gray scales in units of d_{bulk}, relative to the average z position of the plane. (b) Height profiles through the most corrugated and least corrugated surface areas.

in DFT-LDA. In PBE, the reconstructed surface energies are even slightly lower: for Pt, $\Delta E_{5\times N}=0.11$ eV/1×1 (PBE) is in remarkably close agreement with experiment [0.12 ± 0.02 eV/1×1 (Ref. 44)], and we recall that we would expect a further lowering by ≈0.01 eV/1×1 for the theoretical value from relaxation beyond the second layer, as indicated by (5×1) approximants with thicker slabs (see Ref. 56). We thus conclude that *there is no contradiction between theory and experiment for Pt(100)* and that *the reconstruction energies of Au(100) and Pt(100) are similar when the same in vacuo conditions are applied*. In our view, the seeming agreement for Au(100)-(5×1) theory *in vacuo* and electrochemical experiments was accidental.

We next consider the energy difference between the partially and fully rotated approximants in Figs. 1(b) and 1(c) for Au(100) in LDA at the optimum packing density (5×20). The energy gain amounts to 4 meV/1×1 in favor of the approximant closest to experiment, Fig. 1(c). Between a completely unrotated (5×20) cell and the uniformly rotated cell of Fig. 1(c), the change would be 8 meV/1×1. This number is still significant when taken per reconstructed unit cell but is also an order of magnitude smaller than the full reconstruction energy. It is thus fully consistent with the observation that the hex plane can be *modified* depending on its environment[3,39] without disrupting the reconstruction *per se* and gives a quantitative idea of the energy scale of these processes.

In Table I of the accompanying Ref. 56, we demonstrate the excellent agreement of the overall reconstruction geometry calculated here with experimental characteristics available in the literature. Specifically we find a 32% (29%) buckling of the reconstructed top layers for Au(Pt), in units of the bulk interlayer spacing, and an expansion of the layer-averaged top interlayer spacing to 121% (120%). With 4.4% (4.2%), the second layer buckling is much smaller, and only an insignificant contraction of the averaged second-to-third layer spacings by 1% is found. To illustrate the consequences for local surface structure variations, Fig. 3 shows a top view (hex layer only) of the "(5×20)" reconstructed Au(100) surface in LDA. Qualitatively, this picture looks strikingly similar to published atomically resolved STM images.[29] For a more quantitative view, the frame below displays the z coordinate of atomic zigzag rows in the "5" direction with the largest and smallest corrugation amplitude, respectively. The variation shows that very different local environments exist in the surface as a result of the two-dimensional reconstruction. The maximum corrugation in the "5" direction is 0.65 Å (32% of the bulk interlayer spacing d_{bulk}), compared to only 15% in the least corrugated area. These numbers are very similar in LDA and PBE and also very similar to Pt(100)-(5×25) (29% and 14%, respectively). It is precisely such different local environments that drive the preferential nucleation and nanostructuring phenomena on such surfaces.[6–10]

Finally, we turn briefly to the electronic-structure changes that accompany the reconstruction, which we can address directly; such changes are the basis to understand the role of catalytic activity in 5*d* based systems.[6] For 5*d* metals, relativity enhances the participation of the valence *d* electrons by shifting them upwards toward the *s* levels.[57,58] Since *d* electrons are thus more easily promoted to *sp*-type states, enhanced *sp* bonding has been proposed as a cause of the reconstruction.[59,60] On the other hand, enhanced bonding among the *d* states themselves was favored in Ref. 42. Table I shows the shift of the valence-band centers of the surface layer projected densities of states of Ir(100), Pt(100), and Au(100) (all three reconstruct) and Au(100) without relativity, or Ag(100) (the latter two surfaces would not reconstruct), when going from a (1×1) to a (5×1) reconstruction. In short, a characteristic downward shift of the valence-band center occurs for surfaces that reconstruct but is much smaller for the other two surfaces. An additional angular momentum decomposition of the changes shows only a tiny transfer of electrons between the *d* and *sp* channels so the

TABLE I. Valence band center shift of the projected densities of states (LDA) of the surface atoms between (100)-(1×1) and (5×1) hex approximants, for various elements, compared to the computed reconstruction tendency. Au(NR) denotes Au but with a nonrelativistic kinetic energy.

Material	Ir	Pt	Au	Au(NR)	Ag
Actual reconstruction	5×1	Hex	Hex	None	None
Band center shift (eV)	−0.19	−0.24	−0.13	−0.01	−0.08

associated change must happen within the *d* states themselves. Taken together, this analysis thus supports the relativistically enhanced *d-d* hybridization mechanism suggested by TCH (Ref. 42) over *sp* promotion.[59,60]

In conclusion, we have demonstrated that large reconstruction approximants are indeed necessary to capture the subtle reconstruction energy balance of Au(100)-hex and Pt(100)-hex quantitatively. Together with the increasing power of computers and computational methods, realistically large simulations of chemical processes in the presence of reconstruction/deconstruction are now within reach.

This work was funded in part by the EU's Sixth Framework Programme through the NANOQUANTA (Grant. No. NMP4–CT-2004–500198) network of excellence and the EU's Seventh Framework Programme through the European Theoretical Spectroscopy Facility e-Infrastructure (Grant No. 211956).

*Present address: Dept. of Applied Physics, Aalto University, Helsinki, Finland.

[1] *Encyclopedia of Electrochemistry*, edited by A. J. Bard and M. Stratmann (Wiley-VCH, Weinheim, 2006) Vols. 7a-7b.
[2] G. C. Bond *et al.*, *Catalysis by Gold* (Imperial College Press, London, 2006).
[3] C. A. Lucas *et al.*, J. Am. Chem. Soc. **131**, 7654 (2009).
[4] M. Labayen *et al.*, Nature Mater. **2**, 783 (2003).
[5] K. Krug *et al.*, Phys. Rev. Lett. **96**, 246101 (2006).
[6] A. E. Baber *et al.*, ACS Nano **4**, 1637 (2010).
[7] W.-C. Lin *et al.*, Nanotechnology **21**, 015606 (2010).
[8] M. Corso *et al.*, ACS Nano **4**, 1603 (2010).
[9] C. S. Casari *et al.*, Phys. Rev. B **79**, 195402 (2009).
[10] O. S. Hernán *et al.*, Appl. Phys. A: Mater. Sci. Process. **66**, S1117 (1998).
[11] D. Wilgocka-Ślęzak *et al.*, Phys. Rev. B **81**, 064421 (2010).
[12] E. Mateo-Martí *et al.*, Langmuir **26**, 4113 (2010).
[13] L. Gao *et al.*, Phys. Rev. Lett. **101**, 197209 (2008).
[14] K. Suto *et al.*, Langmuir **22**, 10766 (2006).
[15] R. Imbihl, Surf. Sci. **603**, 1671 (2009).
[16] L. Lafferentz *et al.*, Science **323**, 1193 (2009).
[17] C. Bombis *et al.*, Angew. Chem. Int. Ed. **48**, 9966 (2009).
[18] M. Alemani *et al.*, J. Phys. Chem. C **112**, 10509 (2008).
[19] C. Dri *et al.*, Nat. Nanotechnol. **3**, 649 (2008).
[20] H. W. Zandbergen *et al.*, Phys. Rev. Lett. **98**, 036103 (2007).
[21] M. S. Pierce *et al.*, Phys. Rev. Lett. **103**, 165501 (2009).
[22] S. Hagstrom *et al.*, Phys. Rev. Lett. **15**, 491 (1965).
[23] D. G. Fedak and N. A. Gjostein, Phys. Rev. Lett. **16**, 171 (1966).
[24] G. A. Somorjai, Surf. Sci. **8**, 98 (1967).
[25] H. P. Bonzel and R. Ku, J. Vac. Sci. Technol. **9**, 663 (1972).
[26] J. Perdereau *et al.*, J. Phys. F: Met. Phys. **4**, 798 (1974).
[27] A. R. Sandy *et al.*, Phys. Rev. Lett. **68**, 2192 (1992).
[28] G. Binnig *et al.*, Surf. Sci. **144**, 321 (1984).
[29] G. Ritz *et al.*, Phys. Rev. B **56**, 10518 (1997).
[30] M. Chen *et al.*, Science **310**, 291 (2005).
[31] V. Blum *et al.*, Phys. Rev. B **59**, 15966 (1999).
[32] K. Yamazaki *et al.*, Surf. Sci. **199**, 595 (1988).
[33] D. Gibbs *et al.*, Phys. Rev. B **42**, 7330 (1990).
[34] D. Gibbs *et al.*, Phys. Rev. Lett. **67**, 3117 (1991).
[35] D. L. Abernathy *et al.*, Phys. Rev. B **45**, 9272 (1992).
[36] D. L. Abernathy *et al.*, Surf. Sci. **283**, 260 (1993).
[37] P. W. Palmberg, in *The Structure and Chemistry of Solid Surfaces*, edited by G. A. Somorjai, (Wiley, New York, 1969), pp. 29–1.
[38] P. Heilmann *et al.*, Surf. Sci. **83**, 487 (1979).
[39] M. Moiseeva *et al.*, Surf. Sci. **603**, 670 (2009).
[40] P. W. Palmberg and T. N. Rhodin, Phys. Rev. **161**, 586 (1967).
[41] J. Perdew, K. Burke, and M. Ernzerhof, Phys. Rev. Lett. **77**, 3865 (1996).
[42] N. Takeuchi *et al.*, Phys. Rev. B **43**, 14363 (1991).
[43] E. Santos and W. Schmickler, Chem. Phys. Lett. **400**, 26 (2004).
[44] W. A. Brown *et al.*, Chem. Rev. **98**, 797 (1998).
[45] Y. Y. Yeo *et al.*, Science **268**, 1731 (1995).
[46] Y. Y. Yeo *et al.*, J. Chem. Phys. **104**, 3810 (1996).
[47] C. S. Chang *et al.*, Phys. Rev. Lett. **83**, 2604 (1999).
[48] P. van Beurden and G. J. Kramer, J. Chem. Phys. **121**, 2317 (2004).
[49] N. A. Deskins *et al.*, J. Chem. Phys. **122**, 184709 (2005).
[50] Y. J. Feng *et al.*, Phys. Rev. B **72**, 125401 (2005).
[51] T. Jacob, Electrochim. Acta **52**, 2229 (2007).
[52] S. Venkatachalam *et al.*, Chem. Phys. Lett. **455**, 47 (2008).
[53] G. Kresse and J. Furthmüller, Comput. Mater. Sci. **6**, 15 (1996).
[54] V. Blum *et al.*, Comput. Phys. Commun. **180**, 2175 (2009).
[55] V. Havu *et al.*, J. Comput. Phys. **228**, 8367 (2009).
[56] See supplementary material at http://link.aps.org/supplemental/10.1103/PhysRevB.82.161418 for additional information on technical choices, numerical convergence, and computed surface geometry characteristics compared to the literature.
[57] J. P. Desclaux and P. Pyykkö, Chem. Phys. Lett. **39**, 300 (1976).
[58] P. Pyykkö, Angew. Chem. Int. Ed. **43**, 4412 (2004).
[59] T. N. Rhodin *et al.*, in *The Structure and Chemistry of Solid Surfaces*, edited by G. A. Somorjai, (Wiley, New York, 1969), pp. 22–1.
[60] J. F. Annett and J. E. Inglesfield, J. Phys.: Condens. Matter **1**, 3645 (1989).